

X-ray emission from nearby M-dwarfs: the super-saturation phenomenon

David J. James,^{1,2★} Moira M. Jardine,¹ Robin D. Jeffries,³ Sofia Randich,⁴
Andrew Collier Cameron¹ and Miguel Ferreira^{1,5}

¹*School of Physics and Astronomy, North Haugh, University of St Andrews, St Andrews, Fife KY16 9SS*

²*Observatoire de Genève, Chemin des Maillettes 51, CH-1290 Sauverny, Switzerland*

³*Department of Physics, Keele University, Keele, Staffordshire ST5 5BG*

⁴*Osservatorio Astrofisico di Arcetri, Largo E. Fermi 5, 50125 Firenze, Italy*

⁵*Departamento de Ciências Agrárias, Universidade dos Açores, Portugal*

Accepted 2000 June 27. Received 2000 June 5; in original form 2000 February 25

ABSTRACT

A rotation rate and X-ray luminosity analysis is presented for rapidly rotating single and binary M-dwarf systems. X-ray luminosities for the majority of both single and binary M-dwarf systems with periods below $\approx 5\text{--}6$ d (equatorial velocities, $V_{\text{eq}} \gtrsim 6 \text{ km s}^{-1}$) are consistent with the current rotation-activity paradigm, and appear to saturate at about 10^{-3} of the stellar bolometric luminosity.

The single M-dwarf data show tentative evidence for the super-saturation phenomenon observed in some ultra-fast rotating ($\gtrsim 100 \text{ km s}^{-1}$) G- and K-dwarfs in the IC 2391, IC 2602 and Alpha Persei clusters. The IC 2391 M star VXR60b is the least X-ray active and most rapidly rotating of the short period ($P_{\text{rot}} \lesssim 2$ d) stars considered herein, with a period of 0.212 d and an X-ray activity level of about 1.5 sigma below the mean X-ray emission level for most of the single M-dwarf sample. For this star, and possibly one other, we cautiously believe that we have identified the first evidence of super-saturation in M-dwarfs. If we are wrong, we demonstrate that only M-dwarfs rotating close to their break-up velocities are likely to exhibit the super-saturation effect at X-ray wavelengths.

The M-dwarf X-ray data also show that there is no evidence for any difference in the X-ray behaviour between the single and binary systems, because for the single stars, the mean $\log L_x/L_{\text{bol}} = -3.21 \pm 0.04$ ($0.2 \lesssim P_{\text{rot}} \lesssim 10.1$ d), whereas for the binary stars, the mean $\log L_x/L_{\text{bol}} = -3.19 \pm 0.10$ ($0.8 \lesssim P_{\text{rot}} \lesssim 10.4$ d).

Furthermore, we show that extremely X-ray active M-dwarfs exhibit a *blue excess* of about 0.1 magnitudes in $U\text{--}B$ compared with less active field M-dwarfs. Such an excess level is comparable to that observed for extremely chromospherically active M-dwarfs. Moreover, as is the case for M-dwarf Ca II H and K activity levels, there is an *exclusion zone* of X-ray activity between the extremely active M-dwarfs and the less active ones.

Key words: stars: activity – stars: late-type – stars: rotation – X-rays: stars.

1 INTRODUCTION

It is now widely believed that radiative losses from the outer atmospheres of solar-type stars (spectral types late-F \rightarrow M) are produced by confinement and heating of stellar plasma in complex magnetic field structures above their surfaces (Schwarzschild 1948; Ulmschneider 1967; Rosner, Tucker & Vaiana 1978a; Rosner et al. 1978b; Heyvaerts & Priest 1983). Optical, UV, EUV and X-ray observations of solar-type, low-mass stars, both in the field and young ($\lesssim 700$ Myr) open clusters, have provided

evidence for a correlation of increased magnetic activity manifestations (e.g. H α , Ca II H and K, Mg II H and K and X-ray fluxes) with increasing rotation rate (e.g. Vilhu 1984; Noyes et al. 1984; Doyle 1987; Soderblom et al. 1993, hereafter S93; Stauffer et al. 1994; Randich et al. 1996). The so-called rotation-activity paradigm evident from such observations is most likely a consequence of the stellar *dynamo* process, which converts motions of conducting plasma, in the remnants of a presumably relic field, into electric currents and induced magnetic fields. These field lines are supposed to be *frozen* into the conducting plasma (Ferraro 1937), and the relic field lines threading the stellar convective zone are twisted, stretched and deformed by the

★ E-mail: djj@st-and.ac.uk

interaction of differential rotation and convective motions leading to the regeneration and enhancement of the existing magnetic field.

The efficiency of the stellar dynamo is related to both the rotation period, P , and the convective turnover time, τ_c , through the Rossby number ($R_0 = P/\tau_c$). Magnetic flux, and hence magnetic activity induced emissions, increase with decreasing Rossby number (and as τ_c is large in lower mass stars, the dynamo is expected to be more efficient in the lower mass of two stars having identical rotation periods). However there are observational data which suggest, at first glance, that the dynamo process does not continue to operate *ad infinitum*, but saturates above some limiting rotational velocity (or below a fiducial Rossby number). The data quite clearly show that for late-type stars rotating above $\approx 15\text{--}20\text{ km s}^{-1}$ (more like $5\text{--}8\text{ km s}^{-1}$ for M-dwarfs), a saturation-like plateau in the observed chromospheric and coronal emissions is measured (Vilhu & Walter 1987; S93; Stauffer et al. 1994, 1997). The saturated X-ray emission plateau is characterized by X-ray luminosities at about 10^{-3} of the stellar bolometric luminosities. Moreover, saturation-like emission plateaux are also observed in chromospheric and transition region lines, although the evidence is less compelling than that for coronal emission (Vilhu & Walter 1987; S93; James & Jeffries 1997); nonetheless, saturation of the radiative losses from relatively rapidly rotating late-type stars appears to be occurring from all levels of their outer atmospheres.

Surprisingly perhaps, the IC 2391, IC 2602 and Alpha Persei open clusters show a downward trend from a saturated X-ray emission plateau – termed super-saturation – for a few G- and K-dwarf members with extremely high rotation rates ($v \sin i \sim 100\text{--}200\text{ km s}^{-1}$, or $\log R_0$ between -1.8 and -2.0 , (Prosser et al. 1996; Randich 1998). Unfortunately there are too few stars in these authors’ samples exhibiting super-saturation to say whether this occurs at a given rotation rate or specific Rossby number. This is especially apparent for the Rossby number range as the Randich (1998) Rossby numbers are taken from Stauffer et al. (1997), who in turn use rotation period estimates using a projected equatorial velocity ($v \sin i$) and a mean inclination angle of $4/\pi$. However a *lower* limit for equatorial velocities of about 100 km s^{-1} for super-saturation to occur in these stars can be inferred from their $v \sin i$ values. Similarly, this equates to a *upper* limit of Rossby number for super-saturation of around -1.40 (see Section 4).

The physical cause of the super-saturation (and indeed saturation!) of stellar X-ray emission is far from being fully understood. It is possible that the dynamo itself is self-limiting, maybe via a Lorentz back-reaction and shear stresses across field boundaries (Charbonneau & MacGregor 1992), or that a saturation of the magnetic heating processes which energize coronal plasma is occurring in the most rapidly rotating stars. However, O’Dell et al. (1995) discuss arguments that it is not the dynamo that is saturating but the star-spot activity (under the assumption that spot coverage acts as a tracer for the total surface magnetic flux). They present differential photometry data which indicate that star-spot activity (and hence surface magnetic flux) in solar-type stars saturates at a rotation at least 6–10 times at that inferred from chromospheric and coronal flux data. Such a hypothesis is given credence by the theoretical work of Solanki, Motamen & Keppens (1997), who show that rapid rotation leads to the concentration of magnetic flux near the poles of rapidly rotating solar-type stars. Such regions will act to mimic the saturation of magnetic activity indicators by creating more open-field regions (reducing the trapping and heating of upper atmosphere plasma). This effect

also provides an acceptable alternative for stellar spin-down models which require dynamo saturation to fit the rotation-age data for young open clusters.

An alternative hypothesis is that the X-ray emitting coronal volume of rapid rotators is reduced via centrifugal stripping (e.g. Jardine & Unruh 1999). As the stellar rotation rate increases, centrifugal forces cause a rise in the pressure and density in the outer parts of the largest magnetic loops, predisposing them to prominence formation at the corotation radius. This process stresses and distorts the field, opening up previously closed field lines (destroying X-ray emitting regions) when the prominences erupt. Jardine & Unruh showed that if the extent of the corona is limited by the corotation radius, then X-ray saturation and super-saturation occur naturally for G stars, without the need for dynamo saturation.

The models of Jardine & Unruh (1999) show that for increasing rotation rate in G-dwarfs (their fig. 1), coronal temperatures increase quite considerably (up to an order of magnitude or more). If their models mirror some degree of physical reality, we must then also consider the possibility that rapid rotators may sustain sufficiently hotter coronae such that the *ROSAT* observatory can no longer measure the peak of their emission distributions in its relatively narrow 0.1–2.4 keV passband (see also Randich 1998). While there is no evidence that coronal temperatures of late-type stars behave anywhere near such extremes as ten-fold increases in coronal temperatures for X-ray active stars compared to low activity stars, there is evidence of some temperature difference between the coronae of X-ray active and more inactive late-type stars. Gagné, Caillault & Stauffer (1995) have provided analyses of X-ray data for G-, K- and M-dwarf Pleiads which show that single- and two-temperature plasma model fits to the data both yielded moderately hotter coronal temperatures for the more rapidly rotating G and M stars in their sample. While we accept there may be some effect from a likely temperature shift in the coronae of rapid rotators, we do not believe such an effect can produce the required shift in the peak emission measure to explain the observed super-saturation in the rapid rotators (see Section 4), and some or other hypotheses must be more fully explored.

We wish to investigate whether super-saturation occurs at a given period, rotation speed or Rossby number and thus gain some insight into the physical mechanism that causes it. The key to such an investigation is to sample the extremes of *both* rotation rate and convection zone depth. For this reason we present an analysis of a sample of single and binary M-dwarfs, with thick convection zones, and compare their behaviour with the rapidly rotating, super-saturated G- and K-dwarfs in the IC 2391 and Alpha Per clusters. The paper is structured as follows: in Section 2, the physical data, and their sources, are listed for our sample together with the analysis procedures adopted. We present the results in Section 3, while a fuller discussion of the data and their implications are deferred to Section 4. Finally, we summarize and conclude our findings.

2 THE SAMPLE AND DATA PROCESSING

A sample of rapidly rotating single and binary M-dwarfs has been assembled from a variety of literature searches and the SIMBAD database. All single stars were chosen such that their photometric rotation periods were known, and a *ROSAT PSPC* X-ray observation existed for each. The binary stars were chosen rather more selectively. Their rotation periods are inferred from the

spectroscopically determined orbital motion of the binary under the assumption that each component of the binary system is tidally locked to its companion through a tidal coupling of its orbital and rotational motion (for orbital periods of ~ 10 d or less – Zahn 1977, 1989). Binary M-dwarf systems were therefore chosen having periods of ~ 10 d or less, and if a *ROSAT* X-ray observation existed for each system.

Physical data for the single and binary M-dwarfs are presented in Tables 1–3. All available V , $B-V$ and $V-I$ (Kron or Cousins systems) photometric data for the single and binary systems are listed in Table 1. The various sources of the data are given in column 6. For some systems only $V-I_K$ data are available. These data were transformed onto the Cousins system using the $V-I_K$, $V-I_C$ relationship presented in Bessel & Weis (1987). X-ray data are presented in Tables 2 and 3 for single and binary M-dwarfs, respectively. X-ray flux has been divided equally between binary components. Apart from the Alpha Per (AP) stars ($E_{V-I_C} = 0.125$), the IC 2602 (R) stars ($E_{V-I_C} = 0.04$) and the IC 2391 (VXR) stars ($E_{V-I_C} = 0.01$), negligible reddening is assumed for all the remaining single and binary stars. Systematic errors in the various X-ray datasets can be reduced by removing the uncertainties in stellar distance by using L_x/L_{bol} as the X-ray activity parameter. The calculation of bolometric luminosities for M stars is obviously sensitive to the choice of bolometric corrections (BC). The usual method for solar-type stars is to use a $B-V$ colour relation. However, the $B-V$ colours of M-dwarfs are relatively insensitive to temperature, and so one must use the $V-I$ colour to determine bolometric corrections. The BC for all stars presented in Tables 2 and 3 are calculated using equation (6) from Monet et al. (1992) and the Cousins $V-I$ photometric data. For all

Table 1. For all single and binary field M-stars (ie non-cluster stars) listed in Tables 2 and 3, observed V , $B-V$, $V-I_K$ and $V-I_C$ photometric data are presented in columns 2–5, respectively. Sources of the data are listed in column 6. The stars with entries in the $V-I_K$ columns do not have $V-I_C$ data available, and the tabulated $V-I_C$ values are determined from the $V-I_K$, $V-I_C$ relationship presented in Bessel & Weis (1987).

Star	V	$B-V$	$V-I_K$	$V-I_C$	Ref
Gl 182	10.05	1.40	–	1.83	A
Gl 285	11.19	1.6	–	2.95	A
Gl 388	9.28	1.54	–	2.50	B
Gl 411	9.47	1.51	–	2.15	B
Gl 551	11.11	1.97	–	3.67	A
Gl 803	8.73	1.45	–	2.06	C
Gl 873	10.23	1.61	2.57	2.68	D
Gl 875.1	11.62	1.46	2.38	2.51	E
RE1816+541	11.83	1.45	–	2.01	F
Gl 890	10.84	1.42	–	1.84	A
HD 16157	8.81	1.36	–	1.86	G
Gl 268	11.48	1.72	2.97	3.04	E
FF And	10.53	1.50	1.95	2.10	D
YY Gem	9.09	1.42	–	1.87 $^{\alpha}$	H
CM Dra	12.90	1.53	–	2.92	A, I
FK Aqr	9.09	1.46	–	2.19	J
RX J0222.4+4729	11.10	1.44	–	1.74	K
Gl 841a	10.45	1.49	–	2.38	L

NOTES: α – determined from a $V-I$ (Johnson) = 2.40. It has been transformed to the Cousins system using the relationship, $V-I_C = 0.835(V-I)_j - 0.13$ [for $2 < (V-I)_j < 3$ – Bessel 1979].

Refs: A: Bessel (1990); B: Celis (1986); C: Cutispoto (1998a); D: Weis (1993); E: Weis (1996); F: Schwartz et al. (1995); G: Cutispoto (1998b); H: Barnes, Evans & Moffet (1978); I: Eggen (1986); J: Cutispoto & Leto (1997); K: Chevalier & Ilovaisky (1997); L: Laing (1989).

binary systems, the bolometric luminosity has been calculated assuming the V magnitude is 0^m.75 dimmer (assumes equal mass components).

Spectral-type data for all single and binary stars are taken from the photometric references in Table 1 and/or the SIMBAD database and references therein. For the three Alpha Persei stars (AP) only $V-I$ Kron values were available. These data were transformed onto the Cousins system using the same $V-I_K$, $V-I_C$ relationship employed for the field stars. Rotation periods for the single stars, column 5 in Table 2, are taken from the following: Gliese star data – Mathioudakis et al. (1995); Alpha Persei (AP) data – Prosser et al. (1993), Prosser & Grankin (1997); IC 2602 (R) data – Barnes et al. (1999), IC 2391 (VXR) data – Patten & Simon (1996), Simon & Patten (1998), whereas the RE1816+541 datum is from Robb & Cardinal (1995). Orbital/rotation periods for the binary M-dwarf sample, column 5 in Table 3, are taken from Jeffries & Bromage (1993), Jeffries et al. (1993), Chevalier & Ilovaisky (1997) and Dempsey et al. (1997). In columns 6 and 7 of Tables 2 and 3 convective turnover times (τ_c) and Rossby numbers (R_0) are presented. Convective turnover times (in days) are calculated from equation (4) presented in Noyes et al. (1984), suitable for stars with $B-V > 1.00$, with an assumed mixing length parameter of $\alpha = 2$. Sources of X-ray detection for the single stars are detailed as footnotes to Table 2. Five separate *ROSAT* PSPC flux conversion factors (CFs) have been used to calculate X-ray fluxes for the single stars, however only minor differences in absolute X-ray flux levels will result.

The source of X-ray detections for the binary M stars is listed in column 8 of Table 3, and all are sources from the *ROSAT* All-Sky Survey. The standard RASS CF has been used for each, and X-ray flux has been divided equally between the binary components. The plots and the discussion do not include the two binary systems RX J0222.4+4729 and HD 16157 because they have unequal mass components and the correct allocation of X-ray and bolometric flux is problematic. Bolometric flux for the remaining binary systems has been calculated assuming two equal mass components. Gliese 866 and Gliese 570B have not been included in the sample due to their long periods of rotation (2.2 yr and 309 d, respectively). DF UMa has also been excluded because the system parameters are not fully understood, especially the spectral type of the secondary. The recent discovery of the new M-dwarf eclipsing binary GJ 2069A has also been excluded because it is believed to be in a quadruple system of M-dwarfs, with another M-dwarf binary GJ 2069B (see Delfosse et al. 1999), and the allocation of X-ray flux is problematic. Although RE0618+75 is an excellent candidate ($P_{rot} = 0.539$ d – Jeffries et al. 1993), there are no presently available photometric data for this system.

3 RESULTS

X-ray luminosities, as a fraction of bolometric luminosities, are plotted against rotation period and Rossby number for our sample of single and binary M-dwarfs in Figs 1 and 2, respectively. We note that the relatively high datum at $L_x/L_{bol} = 10^{-2.61}$ in both figures is for Gl 873, and is moderately higher than the expected X-ray saturated level of 10^{-3} seen in G-, K- and M-dwarfs both in the field and young open clusters. The PSPC data for Gl 873 have been extracted from the public archive (RP 200984n00 PSPC) and a time-series analysis reveals the presence of a steep increase in X-ray photon count rate during the exposure, most likely indicating a flaring event in the star’s corona. In fact, there already exists evidence that this star is highly X-ray active and

Table 2. Photometric and X-ray data are tabulated for single M-dwarfs in the field and three young (≤ 50 My) open clusters with known rotation periods and X-ray detections. Apart from the Alpha Per (AP) stars ($E_{V-I_C} = 0.125$), the IC 2602 (R) stars ($E_{V-I_C} = 0.04$) and the IC 2391 (VXR) stars ($E_{V-I_C} = 0.01$) ($A_V = 2.68 \times E_{V-I_C}$), negligible reddening is assumed. Bolometric corrections (BC) are determined from the $V-I_C$ data (Monet et al. 1992).

Star	V_0	$(V-I_C)_0$	Spectral type	Period (d)	τ_c (d)	$\log R_0$	X-ray Ref	X-ray count rate (count s $^{-1}$)	HR I	BC	$\log L_x/L_{\text{bol}}^{II}$
Gl 182	10.05	1.83	dM0.5e	4.56	26.18	-0.76	RASS	0.6514 ± 0.0421	-	-1.31	-3.30
Gl 285	11.19	2.95	dM4.5e	2.78	27.93	-1.00	S95	1.4172 ± 0.0727	-0.22	-2.60	-2.95
Gl 388	9.28	2.50	dM4.5e	2.70	27.39	-1.01	S95	3.6709 ± 0.0041	-0.08	-2.04	-3.04
Gl 411	9.47	2.15	dM2e	48.0	27.13	0.25	S95	0.1823 ± 0.0043	-0.63	-1.64	-4.30
Gl 551	11.11	3.67	dM5e	42.0	31.46	0.13	S95	1.4102 ± 0.0591	-0.36	-3.63	-3.45
Gl 803	8.73	2.06	dM0e	4.87	26.61	-0.74	RASS	5.9520 ± 0.1210	-	-1.54	-2.97
Gl 873	10.23	2.68	dM4.5e	4.38	28.02	-0.81	S95	5.2232 ± 0.0956	-0.16	-2.26	-2.61
Gl 875.1	11.62	2.51	dM3.5e	1.64	26.69	-1.21	RASS	0.4689 ± 0.0313	-	-2.05	-3.12
RE1816+541	11.83	2.01	dM2e	0.46	26.61	-1.76	RASS	0.2920 ± 0.0130	-	-1.49	-3.01
Gl 890	10.84	1.84	dM2e	0.44	26.35	-1.78	RASS	0.4266 ± 0.0586	-	-1.32	-3.18
AP 60	15.40	2.40	dM3	0.318	27.93	-1.94	R96	0.0040 ± 0.0010	-	-1.92	-3.10
AP 96	14.21	1.95	dM0	0.346	26.35	-1.88	P96	0.0060 ± 0.0010	-	-1.43	-3.20
AP 211	14.73	1.78	dM0	0.288	26.10	-1.96	P96	0.0038 ± 0.0005	-	-1.26	-3.12
R24A	14.52	1.82	-	1.25	26.10	-1.32	R95	0.0090 ± 0.0010	-	-1.29	-3.07
R26	15.08	2.11	-	5.70	27.04	-0.68	R95	0.0023 ± 0.0006	-	-1.59	-3.56
R31	15.00	2.20	-	0.49	27.48	-1.75	R95	0.0110 ± 0.0010	-	-1.69	-2.95
R32	15.01	2.12	-	4.00	27.84	-0.84	R95	0.0063 ± 0.0009	-	-1.61	-3.15
R44	14.73	1.99	-	5.50	27.13	-0.69	R95	0.0026 ± 0.0007	-	-1.47	-3.59
R50	14.63	2.03	-	6.40	27.21	-0.63	R95	0.0080 ± 0.0010	-	-1.51	-3.16
R53B	15.25	2.45	-	0.41	27.66	-1.83	R95	0.0079 ± 0.0008	-	-1.98	-3.11
R56	13.64	1.56	-	4.10	26.10	-0.80	R95	0.0140 ± 0.0010	-	-1.05	-3.13
R57	15.43	2.40	-	8.70	27.57	-0.50	R95	0.0041 ± 0.0007	-	-1.92	-3.30
R77	14.08	1.68	-	10.10	26.44	-0.42	R95	0.0031 ± 0.0009	-	-1.16	-3.65
VXR38a	13.34	1.57	dK7.5e	2.78	24.87	-0.95	PS96	0.0198 ± 0.0012	-	-1.06	-3.33
VXR41	13.55	1.54	dK7.5e	5.80	25.03	-0.64	PS96	0.0206 ± 0.0011	-	-1.03	-3.22
VXR42a	15.86	2.48	dM3e	1.81	27.39	-1.18	PS96	0.0102 ± 0.0009	-	-2.01	-3.00
VXR47	13.94	2.06	dM2e	0.258	26.52	-2.01	PS96	0.0168 ± 0.0015	-	-1.54	-3.36
VXR64a	15.30	1.82	-	0.543	26.27	-1.68	PS96	0.0060 ± 0.0004	-	-1.29	-3.16
VXR60a	14.43	2.09	-	0.930	26.78	-1.46	PS93	$0.0092 \pm -$	-	-1.57	-3.44
VXR60b	13.82	1.70	-	0.212	25.93	-2.09	PS93	$0.0092 \pm -$	-	-1.18	-3.52

Notes: I – HR: Hardness Ratio; II – X-ray fluxes in the 0.1–2.4 keV *ROSAT* bandpass.

See text for rotation period references.

Sources of X-ray detection are listed in column 8, and are indicated as RASS: *ROSAT* All-Sky Survey; S95: Schmitt, Fleming & Giampapa (1995); R96: Randich et al. (1996); P96: Prosser et al. (1996); R95: Randich et al. (1995); PS96: Patten & Simon (1996); PS93: Patten & Simon (1993).

Five separate *ROSAT* *PSPC* flux conversion factors have been used to calculate X-ray fluxes. The *standard* RASS CF, for negligible interstellar absorption, of 6×10^{-12} erg cm $^{-2}$ count $^{-1}$ has been used for RASS sources. For Schmitt et al. (1995) sources, a CF of $(5.30 \times \text{HR} + 8.31) \times 10^{-12}$ erg cm $^{-2}$ count $^{-1}$ has been used, whereas the CF used for Alpha Persei (AP) stars is 2×10^{-11} erg cm $^{-2}$ count $^{-1}$, and a CF of 1.2×10^{-11} erg cm $^{-2}$ count $^{-1}$ is used for the IC 2602 (R) stars.

For IC 2391 (VXR) stars, the *PSPC* CF used was 7.1×10^{-12} erg cm $^{-2}$ count $^{-1}$.

For four of the IC 2391 stars, 42a, 60a,b, 64a, there are no $B-V$ data values available. To calculate Rossby numbers for these stars, a field-star $V-I$ to $B-V$ relation was first used (Caldwell et al. 1993).

Table 3. Photometric and X-ray data are tabulated for binary M-dwarfs in the field with known rotation periods (below ~ 10 d) and X-ray detections (in the *ROSAT PSPC* 0.1–2.4 keV passband). Negligible reddening is assumed, and bolometric corrections (BC) are determined from the $V-I_C$ data.

Star*	V_0	$(V-I_C)_0$	Spectral type	Period (d)	τ_c (d)	$\log R_0$	X-ray Ref	X-ray count rate $^\alpha$ (count s $^{-1}$)	BC	$\log L_x/L_{\text{bol}}^\beta$
Gl 841a	10.45	2.38	dM3-5e + dM3-5e	1.124	26.95	-1.38	RASS	1.0770 ± 0.0812	-1.90	-3.16
Gl 268	11.48	3.04	dM5e + dM5e	10.43	29.03	-0.44	RASS	0.2570 ± 0.0410	-2.72	-3.70
FF And	10.53	2.10	dM1e + dM1e	2.17	27.04	-1.10	RASS	1.0220 ± 0.0473	-1.58	-3.03
YY Gem	9.09	1.87	dM1e + dM1e	0.81	26.35	-1.51	RASS	3.6970 ± 0.0912	-1.35	-2.95
CM Dra	12.90	2.92	dM4e + dM4e	1.27	27.30	-1.33	RASS	0.1767 ± 0.0155	-2.56	-3.23
FK Aqr	9.09	2.19	dM2e + dM3e	4.39	26.69	-0.78	RASS	3.8030 ± 0.1869	-1.68	-3.07
HD 16157	8.81	1.86	dK7 + dM3	1.56	25.85	-1.22	RASS	3.6790 ± 0.2241	-1.34	-3.06
RX J0222.4+4729	11.10	1.74	dM0e + dM5e	0.465	26.52	-1.76	RASS	0.2211 ± 0.0223	-1.21	-3.32

Notes: All X-ray detections are from the *ROSAT* All-Sky Survey and the RASS CF, for negligible interstellar absorption, of 6×10^{-12} erg cm $^{-2}$ count $^{-1}$ has been used. The two systems detailed below the two horizontal lines are included for reference only, and will not be included in the discussion (see text).

α – X-ray flux has been divided equally between the components.

β – Bolometric flux has been calculated using $V + 0^{m75}$ – assuming two equal mass components.

* – Alternative names: FF And \equiv GJ 9022; YY Gem \equiv Gl 278c; CM Dra \equiv Gl 630.1a; FK Aqr \equiv Gl 867a.

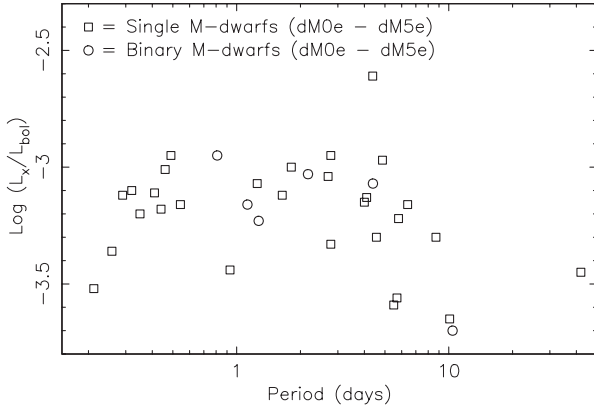


Figure 1. X-ray luminosity, as a fraction of bolometric luminosity, is plotted against rotation period (based on a 24-h day) for the single and binary M-dwarfs considered in the present sample (excludes RX J0222.4+4729 and HD 16157). The moderately high datum (GI 873) at $\log L_x/L_{\text{bol}} = -2.61$ is likely due to a flaring event on the star at the time of the X-ray observations (see text).

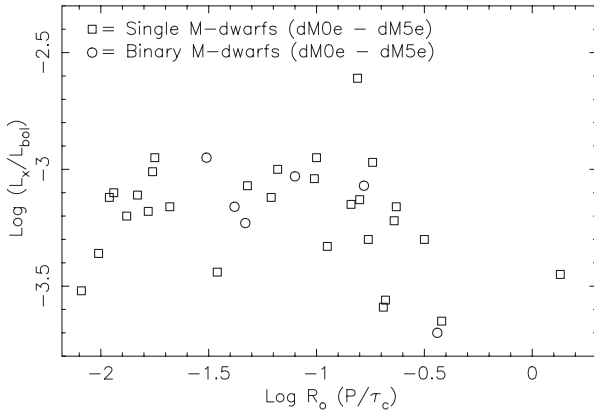


Figure 2. X-ray luminosity, as a fraction of bolometric luminosity, is plotted against Rossby number R_0 ($\equiv P_{\text{rot}}/\tau_c$) for the single and binary M-dwarfs considered in the present sample (excludes RX J0222.4+4729 and HD 16157). There is tentative evidence for the super-saturation effect at $\log R_0 \sim -2.0$, which is also seen in some extremely rapidly rotating IC 2391, IC 2602 and Alpha Persei G- and K-dwarfs ($v \sin i \sim 100\text{--}200 \text{ km s}^{-1}$ and $\log R_0 \sim -2.1$; Prosser et al. 1996; Randich 1998).

indeed shows flaring activity. X-ray data taken with the ASCA observatory show that an intense X-ray flare from the star took place on 1998 July 12, which was as luminous as 25 per cent of its bolometric luminosity and lasted over 3 h (Favata et al. 2000).

Excluding the two slow rotators (periods greater than 40 d) and the highly X-ray active star (GI 873), it is apparent from Figs 1 and 2 that the majority of the remaining single and binary M-dwarfs in the present sample, with periods less than 5–6 d and log Rossby numbers less than -0.7 , are at or about the X-ray saturation level of $L_x/L_{\text{bol}} \sim 10^{-3}$ for rapidly rotating late-type stars. There is tentative evidence of a drop in X-ray activity among the single stars as one moves to longer period systems (≥ 6 d) and higher Rossby numbers ($R_0 \geq -0.7$), which can probably be attributed to a decline in the magnetic dynamo efficiency through the rotation-activity paradigm. The single star and the binary system with periods of about 10 d, both have $\log L_x/L_{\text{bol}}$ values which are several times their standard deviations below their

respective mean values (see below). Unfortunately, there are too few data at or about this period to accurately determine the rotation rate at which any drop from X-ray saturation occurs.

It is evident from Figs 1 and 2 that the data look very similar in period and Rossby number space. This is because the empirical relation of Noyes et al. (1984) used to calculate their convective turnover times flattens-off at $B-V$ values above 1.2 or so. However, the Noyes et al. parameterization gives a perfectly acceptable fit out to $B-V = 1.63$ when compared to X-ray and rotation period data for Hyades members and more modern theoretical stellar models (Pizzolato et al. 1999). Such models yield slightly better fits to the Hyades data, with moderately steeper dependences on $B-V$ colour. However, given that many authors still use the Noyes et al. relation we retain its use here while reminding readers of its potential limitations.

It is also noticeable from Figs 1 and 2 that for systems with periods ≤ 6 d, or $R_0 \leq -0.7$, there is no apparent difference between the X-ray behaviour of single and binary M-dwarfs (excluding RX J0222.4+4729 and HD 16157). This is also apparent statistically, as for single stars (excluding the two systems with periods greater than 40 d and the very X-ray active star, GL 873) the mean $\log L_x/L_{\text{bol}}$ is -3.21 ± 0.04 (error on the mean $-0.2 \leq P_{\text{rot}} \leq 10.1$ d), whereas for binary stars (excluding the two unequal mass systems), the mean $\log L_x/L_{\text{bol}}$ is -3.19 ± 0.10 ($0.8 \leq P_{\text{rot}} \leq 10.4$ d). However, in the absence of error bars for the data, the standard deviations (SD) of the samples are likely to be better estimates of the error for each datum. For the single stars the SD is 0.20, whereas for the binary stars it is 0.25.

At the ultra-fast rotation end of the sample (periods less than 2 d, $R_0 \leq -1.2$), there is considerable scatter in the X-ray level of stars in the sample. The use of differing X-ray CFs amounts to differences of about 0.1 in $\log L_x/L_{\text{bol}}$ space and so not all of the scatter can be attributed to this effect. Varying levels of stellar photospheric spots affecting the $V-I_C$ photometry by differing amounts may have some influence, but again this effect should be really rather small in $\log L_x/L_{\text{bol}}$ space. It is quite conceivable that it is caused by X-ray flaring and/or activity cycles similar to that observed for our Sun. In fact, the observed L_x/L_{bol} scatter is comparable (and perhaps a little less) to that seen in the Hyades and Pleiades clusters (e.g. Stern et al. 1995; Micela et al. 1999).

At $P_{\text{rot}} \leq 0.3$ d or $R_0 \leq -2.0$, there are two data points which show a reduction in X-ray emission compared to the mean, possibly indicating X-ray super-saturation. Furthermore, when one considers that the mean $\log L_x/L_{\text{bol}}$ of the single star sample is -3.21 ± 0.04 , then the least X-ray active ultra-rapid rotator, VXR60b, is about 1.5 sigma below the mean X-ray emission level for the single star sample as a whole. This star is also the fastest rotator in the sample at 0.212 d.

Any probable case for super-saturation in this M-dwarf sample is based on a couple of stars in the ultra-rapid rotator domain. Since the crux of the argument is most likely to be concerned with the X-ray properties of VXR60b, a few words of explanation and discussion are required. Given that both VXR60a and VXR60b are located within the same PSPC detect cell, it is prudent to ask how appropriate it is to divide equally the X-ray flux between the two stars. Both stars are rapidly rotating with periods below 1 d. However, as VXR60a is of lower mass than VXR60b, one may hypothesize which star is the most X-ray active of the two? VXR60a will probably have a more active dynamo than VXR60b, if indeed they are operating within the same parameters, due to its deeper convection zone. But, VXR60b has a greater surface area and therefore it can accommodate more magnetic flux, and hence

support more X-ray emitting regions than VXR60a. Perhaps these two effects cancel each other out to some extent, although if both are saturated and the X-ray flux in each would scale as the bolometric luminosity, then this would mean that VXR60b would be 1.22 times brighter in X-rays than VXR60a.

Even if we were to allocate all of the X-ray flux detected by that PSPC detect cell to VXR60b, what value of L_x/L_{bol} would result? The PSPC count rate of VXR60b would be $0.0184 \text{ count s}^{-1}$ and using the PSPC CF and the relevant bolometric luminosity, an $\log L_x/L_{\text{bol}} = -3.22$ would result. This value lies at the mean of the single star sample as a whole. Of course, it is wholly unreasonable to suggest that VXR60a would not emit substantial X-ray emission of its own due to its rapid rotation, and so VXR60b must sustain an activity of $\log L_x/L_{\text{bol}} > -3.22$. Furthermore, if the total X-ray flux for the VXR60 detect cell is to be shared between star 60a and 60b in the ratios of their bolometric luminosities, then VXR60b would have a PSPC count rate of $0.00101 \text{ count s}^{-1}$ and VXR60a $0.00083 \text{ count s}^{-1}$. These count rates would result in $\log L_x/L_{\text{bol}}$ values of -3.48 for each star. Therefore, whether we divide the VXR60 flux equally between stars VXR60a and VXR60b or divide it according to the ratio of their bolometric fluxes, VXR60b still exhibits a substantially lower X-ray flux than the mean of the single star sample. Moreover, looking at Figs 1 and 2 one can see that the X-ray data for VXR60a place it in a fairly low position relative to all other data with periods less than 2 d. Lowering its X-ray flux even further by sharing the X-ray flux of the VXR60 detect cell between VXR60a and b in the bolometric method above would only serve to lower its L_x/L_{bol} even further making it appear more incongruent with the surrounding data. It is conceivable that its X-ray emission level is indeed higher, moving it more into line with the other data in this region. Allocating more of the X-ray flux from the VXR60 PSPC detect cell to VXR60a would have the effect of *lowering* the X-ray flux for VXR60b further strengthening the argument that it exhibits a super-saturated level of X-ray emission.

There are several M-dwarf data in the single star sample taken from IC 2602 and IC 2391 X-ray studies which have the label A or B associated with their listing, indicating that there is more than one optical counterpart in their X-ray detect error circles. For all these stars except the already discussed VXR60a,b system and the R53 detection, all other associated optical counterparts are photometric non-members of their respective clusters. For the R53 detection, it does indeed have two photometric cluster members inside its PSPC detect cell. However, R53A has a radial velocity of about 5 km s^{-1} away from the cluster mean for IC 2602, and has H α in absorption at a colour where all other members have H α in emission (Stauffer et al. 1997). Hence, this star has doubts cast against its membership of the IC 2602 cluster. We therefore consider R53B as the only cluster member inside that PSPC detect cell and hence allocate all the X-ray flux in that PSPC detect cell to it.

4 DISCUSSION

In order to make a comparison of our data with those of the sample detailed in Randich (1998), one must ensure consistent comparison scales. To assist the reader, we provide the relevant equatorial velocity (V_{eq}) and Rossby numbers for a range of rotation periods for an M2 dwarf, $B-V = 1.50$, $M = 0.39 M_{\odot}$, $R = 0.50 R_{\odot}$ (Zombeck 1990) in Table 4. We are now in a

Table 4. Examples of equatorial velocity (V_{eq}) and Rossby number (R_0) for a range of rotation periods for an M2 dwarf with mass and radius, $M = 0.39 M_{\odot}$, $R = 0.50 R_{\odot}$ (Zombeck 1990).

P_{rot}	V_{eq}	$\log R_0$
(d)	(km s^{-1})	(P_{rot}/τ_c)
10	2.53	-0.43
5.0	5.06	-0.73
1.0	25.3	-1.43
0.5	50.6	-1.73
0.2	126	-2.13

position to interchange discussions referring velocities, period and Rossby numbers with ease.

Possible clues to the cause of super-saturation would be revealed if one could determine the rotation rate or Rossby number at which the decline from X-ray saturation set in; i.e., is rotation the key factor or is there a convection zone depth dependence as well? Given that the solar shell-dynamo models requires both these parameters to function, if one effect is more dominant than the other, the physical mechanism causing super-saturation may become more apparent.

The Alpha Persei, IC2391 and IC2602 sample of G and K stars in the Randich (1998) sample exhibit a decline of X-ray activity from a saturated level at projected equatorial velocities of about 100 km s^{-1} and higher. Given that these measurements contain the unknown projection angle i , it is not possible to say at what velocity this effect becomes apparent. A similar analysis for X-ray activity and Rossby number is presented by Stauffer et al. (1997) using these young open cluster data and those of the Pleiades and Hyades members as well. Their results show that a decline from X-ray saturation sets in at around $\log R_0 \sim -2.0$. However as with the case for $v \sin i$, it is still not possible to ascertain the Rossby number at which super-saturation sets in for G and K stars, because the Stauffer et al. Rossby numbers are calculated from period estimates using the projected equatorial velocity and a mean inclination angle of $4/\pi$. However a *lower* limit for equatorial velocities of about 100 km s^{-1} for super-saturation to occur in these stars can be inferred from their $v \sin i$ values. Similarly, this equates to a *upper* limit of Rossby number for super-saturation of around -1.40 . Therefore, while we cannot infer the exact velocity (or Rossby number) at which super-saturation begins for G and K stars, we can predict a somewhat narrower range of velocities of which it is likely to occur.

4.1 Are M-dwarfs super-saturated at X-ray wavelengths?

In Section 3, we claimed that VXR60b, and to some extent VXR47, provide tentative evidence of super-saturation in M-dwarfs. And, looking at Figs 1 and 2, one can see that the X-ray activity-rotation data for VXR60b appear to lie some way below the mean trend for the remainder of the data. The obvious counter-arguments are that this datum could be erroneous and/or that it is not the only rapidly rotating late-type star in its PSPC detect cell making the true X-ray flux allocation hazardous. Without further observations of VXR60a,b with an X-ray instrument with improved angular resolution it is not possible to correctly determine their relative X-ray levels. Note, the HRI on-board ROSAT was not able

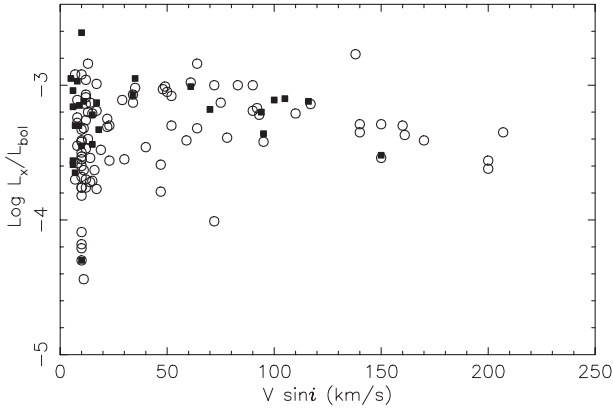


Figure 3. X-ray luminosity, as a fraction of bolometric luminosity, is plotted against projected equatorial velocity ($v \sin i$) for the single M-dwarfs considered in the present sample (solid squares) and for G- and K-dwarfs ($0.60 < V - I_{c,0} < 1.80$) in the IC 2391/2602 and Alpha Persei clusters (open circles). The super-saturation effect is the trend of decreasing X-ray activity seen among extremely rapidly rotating IC 2391, IC 2602 and Alpha Persei G-, and K-dwarfs (Prosser et al. 1996; Randich 1998). The M-dwarfs detailed herein appear to follow a similar trend of declining X-ray emission with increasing rotation although there is a paucity of M-dwarf data at higher rotation rates. M-dwarf $v \sin i$ data are taken from the same references as for the rotation period or photometric data and/or the SIMBAD database.

to spatially resolve these two stars (Simon & Patten 1998). However, with rotation periods below 1 d, it is likely that both these stars have extremely active dynamo-induced magnetic activity. The position of VXR60a is at the lower edge of the distribution envelope in X-rays for its period, however the considerable scatter of X-ray emission in the remainder of the period range precludes any necessity to believe that it exhibits unusually low X-ray emission levels.

However, if we plot X-ray emission against $v \sin i$ instead of period for the single M-dwarfs in the present sample, further credibility is lent to the existence of the super-saturation effect. X-ray luminosity, as a fraction of bolometric luminosity, is plotted against projected equatorial velocity for all of the single M-dwarfs considered in the present sample (solid squares) and for G- and K-dwarfs ($0.60 < V - I_{c,0} < 1.80$) in the IC 2391/2602 and Alpha Persei clusters (open circles) in Fig. 3. The evidence for X-ray super-saturation amongst the G- and K-dwarfs of the three young Galactic open clusters is fairly clear to see for $v \sin i \geq 100 \text{ km s}^{-1}$. Moreover, although the present M-dwarf sample data are less abundant in this higher velocity range of the diagram, some semblance of a trend for decreasing X-ray emission with increasing rotation rate is visible for the single M-dwarfs.

If we are to advocate M-dwarf super-saturation then we can say that this effect begins at a comparable projected equatorial velocity ($100\text{--}150 \text{ km s}^{-1}$), and a Rossby number ($\log R_0 \sim -2.0$), to the G- and K-dwarfs in the young clusters. On the other hand, if we choose to claim that the evidence is too weak to believe that the M-dwarfs in the current sample are super-saturated, then it cannot occur at the same rotation rate or Rossby numbers as it does for those G and K stars. Hence, we would be forced to conclude that for rotation periods $\geq 0.212 \text{ d}$, M-dwarfs do not exhibit super-saturation at X-ray wavelengths. And therefore, any subsequent search for M-dwarf X-ray super-saturation would have to centre on stars with periods below $\sim 0.21 \text{ d}$ (equatorial velocities greater than $\sim 130 \text{ km s}^{-1}$). Given

that the break-up periods¹ of an $0.39 M_*$, $0.50 R_*$ M2 dwarf and an $0.47 M_*$, $0.63 R_*$ M0 dwarf are 0.13 and 0.17 d, respectively, we would conclude that X-ray super-saturation from M-dwarfs is so rare as to be essentially unobservable.

If we ascertain that M-dwarfs do show super-saturation then an explanation using the physical properties of the stars should be put forward. Of course, one must be sure that it is indeed an effect of the stellar properties and not the method of measurement. In the introduction, we called the reader's attention to the fact that G- and M-dwarfs in the Pleiades exhibited single- and two-temperature plasma model fits to *ROSAT* X-ray data both yielding moderately hotter coronal temperatures. If one supposes that the super-saturation effect is caused by the peak of the X-ray emission moving out of the $1 \pm 1 \text{ keV}$ *ROSAT* passband, some semblance of a sensible explanation is apparent. However, if one examines the original paper (Gagné et al. 1995) more closely, the case for coronal temperature shifts as an explanation for super-saturation is more doubtful. For the composite X-ray spectrum of many Pleiads of the same spectral type, the higher temperature of their two-temperature plasma model fits increase by only 38 and 21 per cent for the G and M stars, respectively, for those stars with $v \sin i > 16 \text{ km s}^{-1}$. Furthermore, the absolute levels of the increased model temperatures are only $kT = 1.27$ and 1.15 keV for the rapidly rotating G- and M-dwarfs, respectively, which is well within the *ROSAT* passband ($0.1 \rightarrow 2.4 \text{ keV}$). Ultimately, such plasma temperatures are model dependent, and our belief that this effect does not contribute significantly to the super-saturation phenomenon will only be fully resolved when *XMM* or *AXAF* observations ($\sim 0.1 \rightarrow 10 \text{ keV}$ passband) for some of these G-, K- and M-dwarf super-saturated systems are analysed.

We now explore the hypothesis that the X-ray emitting coronal volume of ultra-rapid rotators is reduced via centrifugal stripping, and hence ultra-rapidly rotating stars will show decreased levels of X-ray emission, i.e. super-saturation. As the stellar rotation rate increases, centrifugal forces cause a rise in the pressure and density in the outer parts of the largest magnetic loops. This process can be understood in terms of a simple set of arguments. The density structure of a stellar corona is determined by a balance between pressure gradients and the *effective* gravity g_{eff} which includes both gravitational and centrifugal terms:

$$\nabla p = \rho g_{\text{eff}}, \quad (1)$$

where ∇p is the pressure gradient. In the equatorial plane the effective gravity has only a radial component (r):

$$g_{\text{eff}} = \frac{-GM_*}{r^2} + \Omega^2 r, \quad (2)$$

where Ω is the rotation rate of the star and M_* its mass. We can integrate equation (1) analytically for the case where the corona is isothermal and composed of an ideal gas with $p = \rho k_B T / m_H$ (k_B is the Boltzmann constant and m_H the hydrogen mass). We then have for a star of radius R_*

$$\rho(r, \Omega) = \rho_0(\Omega) e^{P(r)},$$

where

$$P(r) = \frac{m_H}{kT} \left[\frac{GM_*}{R_*} \left(\frac{R_*}{r} - 1 \right) + \frac{\Omega_*^2 R_*^2}{2} \left(\frac{r^2}{R_*^2} - 1 \right) \right]. \quad (3)$$

The density (and pressure) fall off exponentially with height close to the surface, then start to rise again at the corotation radius,

¹ $\Omega_{\text{br}} = (GM_*/4R_*^3)^{1/2}$.

$r_c = (GM_*/\Omega^2)^{1/3}$, where $g_{\text{eff}} = 0$. Eventually, the gas pressure becomes greater than the magnetic pressure and the magnetic field lines may be blown open. This height may be taken as the maximum extent of the corona. As the rotation rate increases, the corotation radius moves closer to the star until it moves inside the maximum extent of the corona. For single G stars, this happens at approximately the same rotation rate at which the X-ray emission saturates. Jardine & Unruh (1999) show that if the true extent of the corona is limited by the corotation radius, then the X-ray emission saturates naturally without the need for dynamo saturation. In essence, this is because the increase in the emission due to the increase in the density with rotation rate is balanced by the decrease in the emitting volume. If the density varies as $n_e \propto p/T$ where $T \propto \Omega$ (Jordan & Montesinos 1991) and from equipartition $p \propto B^2 \propto \Omega^2$ for a simple dynamo prescription, then $n_e \propto \Omega$. If the emitting volume is determined by the corotation radius, then $V \propto r_c^3 \propto \Omega^{-2}$ and so the emission measure $\int n_e^2 dV$ becomes independent of the rotation rate. This argument breaks down once the corotation radius is very close to the surface and it is at this point that Jardine & Unruh found super-saturation.

For M stars, however, with their lower mass and radius, the maximum extent of the corona and the position of the corotation radius will be different. How does this affect the interpretation of the results presented here? To illustrate this, we take the case of an M2 star of mass $M = 0.39 M_\odot$ and radius $R = 0.50 R_\odot$ (Zombeck 1990) and an M0 star of mass $M = 0.47 M_\odot$ and radius $R = 0.63 R_\odot$ (Zombeck) and compare them to the case of a G star of solar mass and radius. At a given rotation rate, the density and pressure scaleheights depend primarily on the first term in the expression for $P(r)$ [equation (3)] and hence on the ratio M_*/R_* . For the M2 star, this is only 0.78 times that for the G star (0.75 times, for the M0 star). As a result the pressure scaleheight will be higher and so if the two stars have the same magnetic field, the corona of the M star will be smaller. At the same time, the corotation radius of the M star will be further from the surface since

$$r_c/R_* \propto \frac{M_*^{1/3}}{R_*} \frac{1}{\Omega^{2/3}} \propto \frac{(M_* R_*)^{1/3}}{V_{\text{eq}}},$$

implying that equatorial velocity is the more important parameter in this model. Hence, at the same period, the position of the corotation radius (r_c/R_*) for the M2 star will be 1.46 times that for the G star (1.23 times, for the M0 star). As a result, we expect that the intrusion of the corotation radius into the closed corona, and hence the onset of super-saturation of the X-ray emission, will occur at shorter periods in M stars than in G stars.

In fact, the position of the corotation radius for the M and G stars will be the same only where the period for the M2 star is $(M_*/R_*^3)^{1/2} = 1.77$ times that for the G star (1.37 times, for the M0 star). Among the G- and K-dwarfs of the Alpha Persei cluster, RS CVn and W UMa systems (Randich 1998, fig 4) super-saturation becomes apparent at $\log P_{\text{rot}} \sim 0.9$, i.e. $P_{\text{rot}} \sim 7.94$ h, at which point the corotation radius is about $1 R_*$ above the stellar surface.

In order for the M2-dwarf used in the example above to have a rotation rate where the corotation radius is around $1 R_*$ above the surface, the star would need to rotate at periods of around 4.49 h (0.19 d) and around 5.80 h, 0.24 d, for the M0 star. With a $V-I_{C,0}$ of 1.70, it is likely that VXR60b is nearer to being an M0 dwarf than an M2 dwarf, and so referring to Table 2 and Fig. 1, one can see that VXR60b has a shorter period than 0.24 d, and exhibit a

lower level of X-ray emission compared to the mean emission levels of the remaining single star sample as a whole (excluding the two very long period systems and Gl 873). In fact the least X-ray active ultra-rapid rotator, VXR60b, is about 1.5 sigma below the mean X-ray emission level of the majority of the single star sample.

Unfortunately, we are not able to state that the super-saturation effect occurs at a given Rossby number for G-, K- and M-dwarfs, and so we still cannot rule out that this is a property of either the dynamo or the stars themselves. Essentially, this is because as the convective turnover time increases, the radius goes down by a similar factor, so that for a given equatorial velocity for either, the Rossby numbers are roughly the same.

An alternative hypothesis for the explanation of magnetic-activity indicator saturation has been suggested, which results in a reduction or absence for the need of magnetic dynamo saturation. This hypothesis is based on the premise that a larger fraction of the energy budget of the radiative losses from rapidly rotating late-type stars is converted into continuum emissions, resulting in a *blue excess* emission in the colours of such stars (e.g. Houdebine et al. 1996; Houdebine & Stempels 1997). Such an effect for the chromospheric activity lines H α and Ca II is predicted by the Houdebine et al. models, and is clearly observed among active field M-dwarfs (for a particularly vivid demonstration of this effect, see fig. 14c of Houdebine & Stempels).

Recently, J. Doyle (private communication) has suggested that a similar effect may be present in the X-ray domain, implying that the more X-ray active M-dwarfs should exhibit a *blue excess* in comparison to less active stars of similar mass. To this end, we plot X-ray luminosity, as a fraction of bolometric luminosity, against $U-B$ colour in Fig. 4 for a sample of nearby field M-dwarfs (spectral type M0V–M4V – open squares) and the single M-dwarfs (with available colours – filled circles) listed in Table 2. The general field star X-ray data are taken from a volume-limited sample (within 7 pc) of M-dwarfs detected in the RASS (Fleming, Schmitt & Giampapa 1995), and the $U-B$ colours of these stars and the X-ray active stars listed in Table 2 are taken from the SIMBAD database. Unfortunately the open cluster stars listed in Table 2 do not have any $U-B$ data available.

For the RASS detected stars, the mean colour is $\langle U-B \rangle = 1.16 \pm 0.02$ (error on mean), whereas for the single M-dwarfs exhibiting saturated levels of X-ray emission listed in Table 2 the mean colour is $\langle U-B \rangle = 1.04 \pm 0.06$ (error on mean, excludes two stars with rotation periods over 40 d). Therefore at X-ray wavelengths, it appears that there is a *blue excess* of about 0.1 magnitudes in $U-B$ for very X-ray active M-dwarfs compared to a less-active field star sample. This is a very similar level of $U-B$ excess found for extremely chromospherically active M-dwarfs (Houdebine & Stempels 1997). Another interesting point of note evident from Fig. 4 is that there is an *exclusion zone* of X-ray activity between $\log L_x/L_{\text{bol}}$ of -3.3 and -4 . This could be due to a lack of data points in the very X-ray active M-star sample detailed in this manuscript. However, a remarkably similar zone is observed for chromospheric activity of M-dwarfs in the Ca II H and K lines. If such behaviour at X-ray wavelengths can be successfully modeled, the requirement of invoking dynamo saturation to explain magnetic activity saturation may be eliminated.

5 SUMMARY

We have presented a rotation rate and X-ray luminosity analyses for rapidly rotating single and binary M-dwarf systems. All

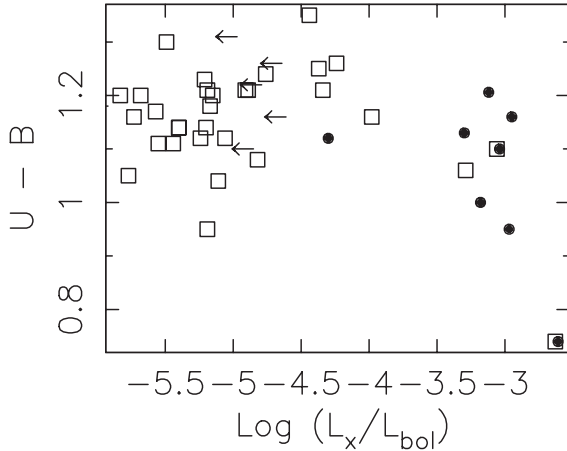


Figure 4. The photometric colour $U-B$ is plotted against X-ray luminosity, as a fraction of bolometric luminosity, for nearby (within 7 pc) M-dwarfs detected in the RASS (data taken from Fleming et al. 1995 – open squares) and the single M-dwarfs (with available colour – filled circles) detailed in Table 2. There is statistical evidence of a *blue excess* (smaller $U-B$ values) in the M-dwarfs with saturated levels of X-ray emission compared to the less-active, nearby field M-dwarfs. It is also clear that there is an *exclusion zone* of X-ray activity, similar to that noted for chromospheric activity of M-dwarfs in the Ca II H and K lines, between $\log L_x/L_{\text{bol}}$ of -3.3 and -4 .

rotation period and X-ray data have been derived from the published literature and the SIMBAD database. The X-ray luminosities for the majority of both single and binary M-dwarf systems with periods below $\approx 5-6$ d (≥ 6 km s $^{-1}$) are consistent with the current rotation-activity paradigm, and appear to saturate at about 10^{-3} of the stellar bolometric luminosity. For the ultra-rapid rotators with rotation periods ≤ 2 d, there is considerable scatter in the X-ray levels observed. This can probably be attributed to magnetic activity cycles, flaring or stellar spots.

The single M-dwarf data show tentative evidence for the super-saturation phenomenon observed in some ultra-fast rotating (100–150 km s $^{-1}$) G- and K-dwarfs in the IC 2391, IC 2602 and Alpha Persei clusters. This supposition is primarily based on one datum for the IC2391 star VXR60b (and possibly VXR 47 as well), a $v \sin i$ -X-ray activity diagram and a theoretical framework which shows a reduction in the coronal volume by coronal stripping should occur at the rotation period of VXR60b. The M-dwarf X-ray data also show that there is no evidence for any difference in the X-ray behaviour between the single and binary systems, because for single stars, the mean $\log L_x/L_{\text{bol}}$ is -3.21 ± 0.04 , whereas for the binary stars, the mean $\log L_x/L_{\text{bol}}$ is -3.19 ± 0.10 .

The hypothesis that the X-ray emitting coronal volume of rapid rotators is reduced via centrifugal stripping has been explored. We demonstrate that an M-dwarf sample would need to incorporate targets with periods of around $P_{\text{rot}} = 5.80$ h (0.242 d) or lower (where the corotation radius is around $1R_*$ above the surface) for X-ray super-saturation to be observed. The IC 2391 star VXR60b is the least X-ray active and most rapidly rotating of the short period ($P_{\text{rot}} \leq 2$ d) systems considered herein, with a period of 0.212 d and exhibits an X-ray activity level about 1.5 sigma below the mean X-ray emission level for most of the single M-dwarf sample. We cautiously believe that we have identified the first evidence of super-saturation in M-dwarfs. If we have not, then only M-dwarfs rotating close to their break up velocities are likely to exhibit the super-saturation effect at X-ray wavelengths.

An analysis of X-ray activity and the $U-B$ colours of M-dwarfs

shows that there is a *blue excess* of about 0.1 magnitudes in $U-B$ for extremely X-ray active stars compared to less active ones. Such an excess level is comparable to that observed for extremely chromospherically active M-dwarfs. This analysis also shows that there is an *exclusion zone* of X-ray activity between the extremely active M-dwarfs and the less active ones, extending over three quarters of a decade in L_x/L_{bol} space.

ACKNOWLEDGMENTS

The provision of advice and electronic data by John Caldwell at the South African Astronomical Observatory and Mike Bessel at Mount Stromlo and Siding Spring Observatory is gratefully acknowledged. This research has made use of the SIMBAD database, operated at the Centre de Données astronomiques de Strasbourg, La France, and the Leicester Database and Archive Service at the Department of Physics and Astronomy, Leicester University, UK. D.J.J. also thanks PPARC for a post-doctoral research fellowship, and the Royal Society for a European research grant. We wish to thank the referee, Dr Gerry Doyle, for his careful reading of the manuscript and the important suggestion of checking the $U-B$ colours. D.J.J. would like to thank Marúa Pilar Escribano Benito for much love and support during this work, and the continued positive influences of Mrs J Pryer. The interesting and varied discussion sessions with Matt Constable, Iain Colwell, Johnnie Jack and Steve Strain were helpful and are gratefully acknowledged.

REFERENCES

- Barnes S. A., Sofia S., Prosser C. F., Stauffer J. R., 1999, *ApJ*, 516, 263
 Barnes T. J., Evans D. S., Moffett T. J., 1978, *MNRAS*, 183, 285
 Bessell M. S., 1979, *PASP*, 91, 589
 Bessell M. S., 1990, *A&AS*, 83, 357
 Bessell M. S., Weis E. W., 1987, *PASP*, 99, 642
 Caldwell J. A. R., Cousins A. W. J., Ahlers C. C., van Wamelen P., Maritz E. J., 1993, *South African Astron. Obser. Cir.*, 15, 1
 Celis S. L., 1986, *ApJS*, 60, 879
 Charbonneau P., MacGregor K. B., 1992, *ApJ*, 387, 639
 Chevalier C., Ilovaisky S. A., 1997, *A&A*, 326, 228
 Cutispoto G., 1998a, *A&AS*, 127, 207
 Cutispoto G., 1998b, *A&AS*, 131, 321
 Cutispoto G., Leto G., 1997, *A&AS*, 121, 369
 Delfosse X., Forveille T., Mayor M., Burnet M., Perrier C., 1999, *A&A*, 341, 63
 Dempsey R. C., Linsky J. L., Fleming T. A., Schmitt J. H. M. M., 1997, *ApJS*, 478, 358
 Doyle J. G., 1987, *MNRAS*, 224, 1p
 Eggen O., 1986, *Catalogue of UBV data*
 Favata F., Reale F., Micela G., Sciortino S., Maggio A., Matsumoto H., 2000, *A&A*, 353, 987
 Ferraro V. C. A., 1937, *MNRAS*, 97, 458
 Fleming T. A., Schmitt J. H. M. M., Giampapa M. S., 1995, *ApJ*, 450, 401
 Gagné M., Caillault J. P., Stauffer J. R., 1995, *ApJ*, 450, 217
 Heyvaerts J., Priest E. R., 1983, *A&A*, 117, 220
 Houdebine E. R., Stempels H. C., 1997, *A&A*, 326, 1143
 Houdebine E. R., Mathioudakis M., Doyle J. G., Foing B. H., 1996, *A&A*, 305, 209
 James D. J., Jeffries R. D., 1997, *MNRAS*, 292, 252
 Jardine M. M., Unruh Y. C., 1999, *A&A*, 346, 883
 Jeffries R. D., Bromage G. E., 1993, *MNRAS*, 260, 132
 Jeffries R. D., Elliott K. H., Kellett B. J., Bromage G. E., 1993, *MNRAS*, 265, 81
 Jordan C., Montesinos B., 1991, *MNRAS*, 252, 21

- Laing J. D., 1989, *South African Astron. Obser. Cir.*, 13, 29
- Mathioudakis M., Fruscione A., Drake J. J., McDonald K., Bowyer S., Malina R. F., 1995, *A&A*, 300, 775
- Micela G. et al., 1999, *A&A*, 341, 751
- Monet D. G., Dahn C. C., Vrba F. J., Harris H. C., Pier J. R., Luginbuhl C. B., Ables H. D., 1992, *AJ*, 103, 638
- Noyes R. W., Hartmann L. W., Baliunas S. L., Duncan D. K., Vaughan A. H., 1984, *ApJ*, 279, 763
- O'Dell M. A., Pnagi P., Hendry M. A., Collier Cameron A., 1995, *A&A*, 294, 715
- Patten B. M., Simon T., 1993, *ApJ*, 415, 123
- Patten B. M., Simon T., 1996, *ApJS*, 106, 489
- Pizzolato N., Maggio A., Micela G., Sciortino S., Ventura P., D'Antona F., 1999, in Pallavicini R., Micela G., Sciortino S., eds, *ASP Conf. Ser. Vol. 178, Stellar Clusters and Associations: Convection, Rotation, and Dynamos*. Astron. Soc. Pac., San Francisco, p. 71
- Prosser C. F., Grankin K. N., 1997, *Noe Observatory Publ.* vol. 1, #3
- Prosser C. F., Schild R. E., Stauffer J. R., Jones B. F., 1993, *PASP*, 105, 269
- Prosser C. F., Randich S., Stauffer J. R., Schmitt J.H.M.M., Simon T., 1996, *AJ*, 112, 1570
- Randich S., 1998, in Donahue R. A., Bookbinder J. A., eds, *10th ASP Conf. Ser. Vol. 154, Cambridge Workshop on Cool Stars, Stellar Systems, and the Sun*. Astron. Soc. Pac., San Francisco
- Randich S., Schmitt J. H. M. M., Prosser C. F., Stauffer J. R., 1995, *A&A*, 300, 134
- Randich S., Schmitt J. H. M. M., Prosser C. F., Stauffer J. R., 1996, *A&A*, 305, 785
- Robb R. M., Cardinal R. D., 1995, *Inf. Bull. Var. Stars*, 4270
- Rosner R., Tucker W. H., Vaiana G. S., 1978a, *ApJ*, 220, 643
- Rosner R., Golub L., Coppi B., Vaiana G. S., 1978b, *ApJ*, 222, 317
- Schmitt J. H. M. M., Fleming T. A., Giampapa M. S., 1995, *ApJ*, 450, 392 [S95]
- Schwartz R. D., Dawkins D., Findley D., Chen D., 1995, *PASP*, 107, 667
- Schwarzschild M., 1948, *ApJ*, 107, 1
- Simon T., Patten B. M., 1998, *PASP*, 110, 283
- Soderblom D. R., Stauffer J. R., Hudon J. D., Jones B. F., 1993, *ApJS*, 85, 315[S93]
- Solanki S. K., Motamen S., Keppens R., 1997, *A&A*, 325, 1039
- Stauffer J. R., Caillault J. P., Gagné M., Prosser C. F., Hartmann L. W., 1994, *ApJS*, 91, 625
- Stauffer J. R., Hartmann L. W., Prosser C. F., Randich S., Balachandran S., Patten B. M., Simon T., Giampapa M., 1997, *ApJ*, 479, 776
- Stern R. A., Schmitt J. H. M. M., Kahabka P. T., 1995, *ApJ*, 448, 683
- Ulmschneider P., 1967, *Z. Astrophys.*, 67, 193
- Vilhu O., 1984, *A&A*, 133, 117
- Vilhu O., Walter F. M., 1987, *ApJ*, 321, 958
- Weis E. W., 1993, *AJ*, 105, 1962
- Weis E. W., 1996, *AJ*, 112, 2300
- Zahn J.-P., 1977, *A&A*, 57, 383
- Zahn J.-P., 1989, *A&A*, 220, 112
- Zombeck M. V., 1990, *Handbook of Space Astronomy and Astrophysics*, 2nd edn. Cambridge Univ. Press, Cambridge

This paper has been typeset from a $\text{\TeX}/\text{\LaTeX}$ file prepared by the author.